Article

Cell Host & Microbe

Bacterial Uracil Modulates *Drosophila* DUOX-Dependent Gut Immunity via Hedgehog-Induced Signaling Endosomes

Graphical Abstract

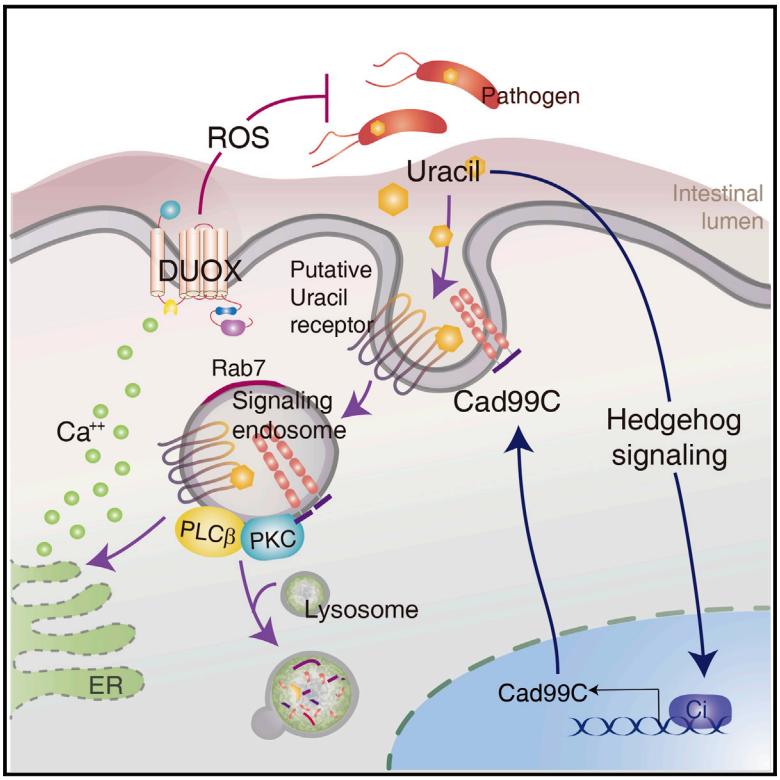

Highlights

- Bacterial uracil induces Hedgehog (Hh) signaling activation in the gut epithelia
- Hh signaling is required for Cad99C-dependent formation of signaling endosomes
- Hh-induced endosomes are required for DUOX activity and ROS generation
- Uracil-induced Hh signaling is required for host resistance to gut infection

Authors

Kyung-Ah Lee, Boram Kim, ..., Daehee Hwang, Won-Jae Lee

Correspondence

lwj@snu.ac.kr

In Brief

Bacterial-derived uracil induces DUOX-dependent microbicidal ROS production in the *Drosophila* gut epithelia through poorly understood mechanisms. Lee et al. show that bacterial uracil induces Hedghog signaling to control Cadherin 99C-dependent signaling endosome formation in enterocytes, which is required for DUOX activation and host resistance to enteric infection.

Lee et al., 2015, Cell Host & Microbe *17*, 191–204
February 11, 2015
http://dx.doi.org/10.1016/j.chom.2014.12.012

Cell Host & Microbe
Article

Bacterial Uracil Modulates *Drosophila* DUOX-Dependent Gut Immunity via Hedgehog-Induced Signaling Endosomes

Kyung-Ah Lee,[1,2,6] Boram Kim,[1,6] Jinhyuk Bhin,[3] Do Hun Kim,[1] Hyejin You,[1] Eun-Kyoung Kim,[1,2] Sung-Hee Kim,[1,2] Ji-Hwan Ryu,[4] Daehee Hwang,[3,5] and Won-Jae Lee[1,2,*]
[1]School of Biological Science, Seoul National University and National Creative Research Initiative Center for Symbiosystem
[2]Institute of Molecular Biology and Genetics
Seoul National University, Seoul 151-742, South Korea
[3]Department of Chemical Engineering, POSTECH, Pohang, Kyungbuk 790-784, South Korea
[4]Research Center for Human Natural Defense System, Yonsei University College of Medicine, Seoul 120-752, South Korea
[5]Department of New Biology and Center for Plant Aging Research, Institute for Basic Science, DGIST, Daegu, 711-873, South Korea
[6]Co-first authors
*Correspondence: lwj@snu.ac.kr
http://dx.doi.org/10.1016/j.chom.2014.12.012

SUMMARY

Genetic studies in *Drosophila* have demonstrated that generation of microbicidal reactive oxygen species (ROS) through the NADPH dual oxidase (DUOX) is a first line of defense in the gut epithelia. Bacterial uracil acts as DUOX-activating ligand through poorly understood mechanisms. Here, we show that the Hedgehog (Hh) signaling pathway modulates uracil-induced DUOX activation. Uracil-induced Hh signaling is required for intestinal expression of the calcium-dependent cell adhesion molecule *Cadherin 99C* (*Cad99C*) and subsequent Cad99C-dependent formation of endosomes. These endosomes play essential roles in uracil-induced ROS production by acting as signaling platforms for PLCβ/PKC/Ca^{2+}-dependent DUOX activation. Animals with impaired Hh signaling exhibit abolished Cad99C-dependent endosome formation and reduced DUOX activity, resulting in high mortality during enteric infection. Importantly, endosome formation, DUOX activation, and normal host survival are restored by genetic reintroduction of *Cad99C* into enterocytes, demonstrating the important role for Hh signaling in host resistance to enteric infection.

INTRODUCTION

Metazoan gut epithelia are in constant contact with diverse microorganisms, ranging from resident symbiotic bacteria to life-threatening pathogens (Lee and Brey, 2013; Ley et al., 2006; McFall-Ngai et al., 2013; Shanahan, 2013). Recent evidence indicates that homeostasis between metazoan gut and gut-associated microbiota regulates a diverse ranges of host physiology, such as immunity, development, and metabolism, while the host, in turn, shapes its microbiota community by modulating gut immunity (Brestoff and Artis, 2013; Hooper et al., 2012; Littman and Pamer, 2011; Ryu et al., 2008). Understanding gut-microbiota interactions is an important undertaking, because the dysregulation of gut-microbe interactions has been shown to lead to severe diseases, including obesity, diabetes, and chronic inflammation (Garrett et al., 2010; Lee and Hase, 2014; Shin et al., 2011; Tremaroli and Bäckhed, 2012; Turnbaugh et al., 2006; Vijay-Kumar et al., 2010; Wen et al., 2008).

Drosophila, with its versatile genetic model and simple commensal community, has been shown to be an excellent genetic model system for investigating these complex reciprocal interactions (Buchon et al., 2013a; Charroux and Royet, 2012; Ferrandon, 2013; Lee and Lee, 2014; Storelli et al., 2011). Evidence shows that *Drosophila* is able to overcome the pathogenic effects from opportunistic pathogens and pathobionts (commensal bacteria that are potentially pathogenic under certain circumstances), while protecting symbionts so as to elicit maximum benefit from them, thereby achieving gut-microbiota homeostasis (Guo et al., 2014; Lee et al., 2013; Lhocine et al., 2008; Paredes et al., 2011; Ryu et al., 2008). Therefore, it is now evident that the host innate immune system plays a critical role in *Drosophila* gut-microbiota homeostasis. Two important innate immune systems are operative in the *Drosophila* gut. Dual oxidase (DUOX, a member of NADPH oxidase family) acts as a first line of the defense system by generating microbicidal reactive oxygen species (ROS) to combat opportunistic pathogens, such as *E. carotovora* (Bae et al., 2010; Ha et al., 2005, 2009b). The immune deficiency pathway (IMD pathway, a *Drosophila* homolog of the mammalian NF-κB pathway) acts as a second line of defense that is responsible for the production of Relish/NF-κB-dependent antimicrobial peptides (AMPs) (Kleino and Silverman, 2014; Lemaitre and Hoffmann, 2007). AMPs are believed to act synergistically and/or complementarily with DUOX-dependent ROS in the regulation of gut-associated microbiota (Ryu et al., 2006). Although both systems are activated in response to bacterial contact, the modes of activation are distinct. The IMD pathway is primarily activated by bacterial-derived *meso*-diaminopimelic acid-type peptidoglycan (PG) (Kleino and Silverman, 2014; Lemaitre and Hoffmann, 2007; Leulier et al., 2003; Royet et al., 2011). In contrast to IMD pathway activation, DUOX is specifically activated by opportunistic

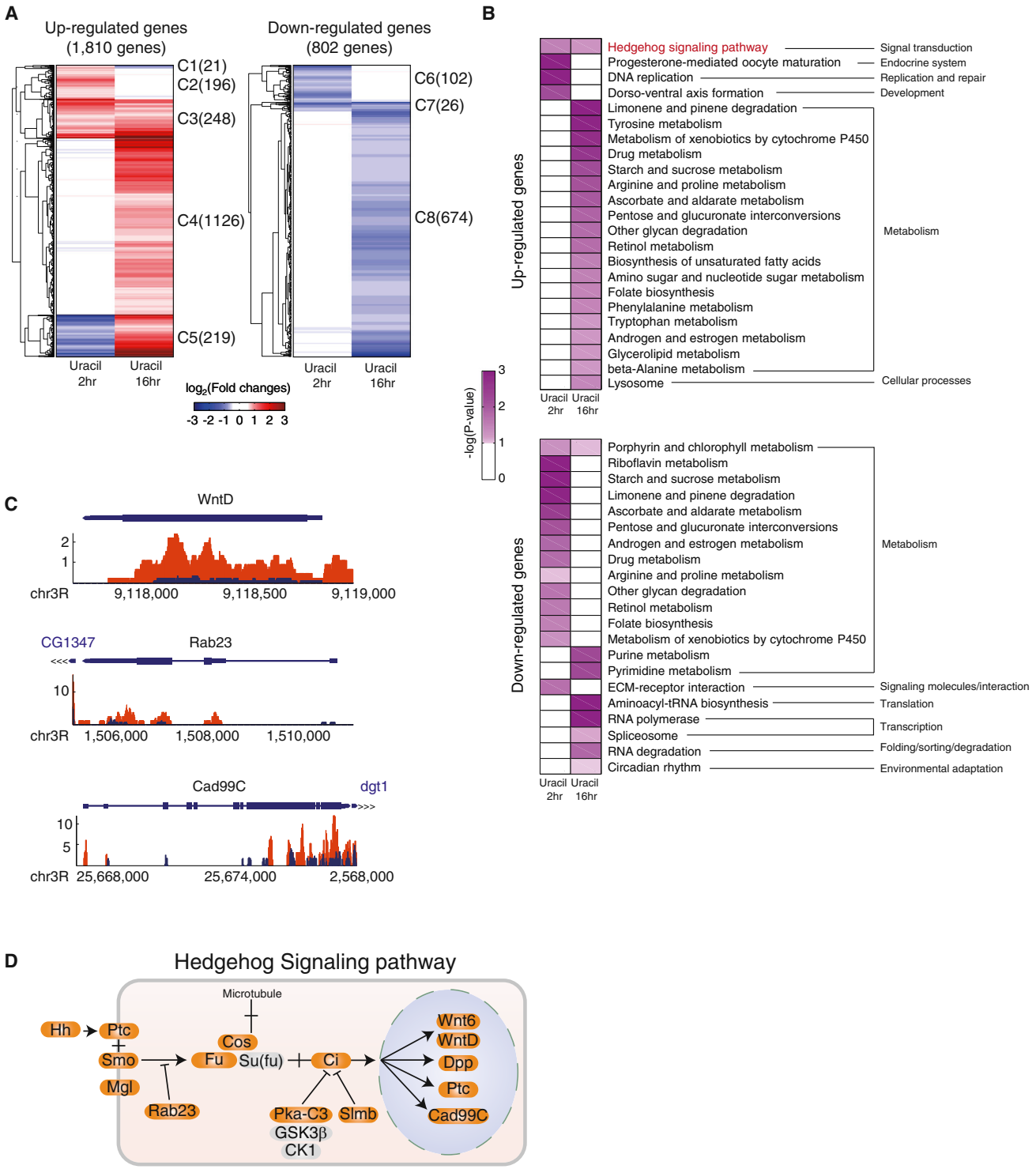

Figure 1. Analysis of mRNA-Sequencing Data Using Anterior Midgut Reveals Hedgehog Signaling as a Major Uracil-Modulated Signaling Pathway

(A) Identification of up- and downregulated genes by uracil treatment. Hierarchical clustering of $\log_2$ fold changes of the uracil-modulated genes at 2 hr (Uracil 2 hr) and 16 hr (Uracil 16 hr) shows five clusters (C1–C5) for upregulated (red) genes and three clusters (C6–C8) for downregulated (blue) genes. Color bar, gradient of $\log_2$ fold changes at 2 or 16 hr.

(B) KEGG pathways represented by the up- and downregulated genes. Color bar, gradient of $-\log_{10}(P)$ where P is the significance of each KEGG pathway being enriched by the up- (upper panel) and downregulated (lower panel) genes.

(legend continued on next page)

pathogens but not symbionts, suggesting a possible role of DUOX in the pathogen-specific activity of the immune system (Bae et al., 2010; Ha et al., 2009b; Lee et al., 2013). Recently, it has been shown that bacterial uracil acts as a DUOX-activating ligand in *Drosophila* gut immunity (Lee et al., 2013). It was further demonstrated that uracil-based DUOX activation plays an essential role in gut immunity and host protection against pathogen infection (Lee et al., 2013). However, despite the central role of uracil as a bacterial-derived ligand in DUOX-dependent gut immunity, the uracil-modulated host signaling pathways remain to be elucidated.

The aim of the present study is to uncover the uracil-induced intracellular signaling pathways and their relationship to DUOX activation in *Drosophila* gut immunity. In this study, the Hedgehog (Hh) signaling pathway was shown to be involved in the formation of *cadherin 99C* (*Cad99C*)-dependent signaling endosomes, which are essential for DUOX-dependent ROS generation and host resistance to gut infection.

RESULTS

Identification of Hh Signaling as a Uracil-Modulated Signaling Pathway

Recently, it was reported that bacterial-derived uracil acts as a ligand for the DUOX activation in the *Drosophila* gut epithelia that is essential for gut-microbe homeostasis (Lee et al., 2013). To gain further insight into uracil-modulated gut immunity, we performed high-resolution RNA-Seq analysis using the *Drosophila* anterior midgut following uracil stimulation. The anterior midgut is one of the intestinal regions most reactive to bacterial challenge and hence a region where DUOX-dependent ROS generation is readily detectable upon microbial or uracil challenge (Lee et al., 2013). A high-resolution transcriptome analysis was undertaken using the Illumina paired-end Hiseq 2000 platform with a read length of 101 nucleotides. On average, 54.7 million sequenced reads were obtained in individual samples and aligned with the *Drosophila* genome (NCBI build 5.3), resulting in 4.5 Giga bps of mapped sequences, representing a 124-fold coverage of the annotated *Drosophila* transcriptome (see Table S1 available online).

The genes exhibiting uracil-induced differential expression at both the early and late time periods following uracil treatment (at 2 or 16 hr, respectively) were categorized into several clusters of 1,810 upregulated genes (C1-C5) and 802 downregulated genes (C6-C8) (Figure 1A; Table S2 and Table S3). For the uracil-modulated genes, we performed functional enrichment analysis based on the Kyoto Encyclopedia of Genes and Genomes (KEGG) pathways (Kanehisa and Goto, 2000). This analysis revealed associations of the uracil-modulated genes with different functional categories, mainly "Metabolism" (Figure 1B; Table S4). Notably, genes involved in different forms of metabolism were downregulated at the early but upregulated at the late time point following uracil treatment (Figure 1B). As expected, RNA-Seq analysis showed that most of the Relish/NF-κB-dependent AMP genes were unaffected at the transcript level by uracil treatment (Table S2 and Table S3), confirming that the uracil-induced signaling pathway and PG-induced IMD-Relish signaling pathway leading to AMP induction are largely independent of one another.

As the initial aim was to identify the uracil-induced signaling pathways that mediate uracil-induced DUOX activation, we focused on the functional category of "Signal Transduction." Functional enrichment analysis revealed that the Hh signaling pathway is a candidate for activation by uracil stimulation (Figures 1B and 1C; Table S4). Among 17 genes involved in the Hh signaling pathway, real-time qPCR analysis found 14 genes were inducible at different time points following uracil treatment (Figures 1D and S1A). Because various uracil-related molecules (other purine and pyrimidine nucleobases as well as eight different pyrimidine analogs) did not induce *Hh* target gene expression (Figure S1B), uracil seems to be a specific ligand for Hh signaling activation. Taken together, the high-resolution RNA-Seq analyses identified Hh signaling as a pathway significantly modulated by uracil in the midgut epithelia.

Hh Signaling Is Required for Uracil-Induced DUOX Activation in the Midgut

To investigate whether uracil indeed induces Hh signaling in the gut, we examined the expression of *Hh* (the Hh signaling ligand) by using *Hh-Gal4 > UAS-GFP*. In the absence of uracil stimulation, we found a high basal level of *Hh* expression in specific regions of the proventriculus and hindgut, with a low yet still considerable basal *Hh* expression in the posterior midgut (Figure 2A). In contrast to other regions, a very low basal *Hh* expression was observed in the anterior midgut region (Figure 2A). Importantly, uracil stimulation rapidly induced *Hh* expression, predominantly in the anterior midgut and the posterior midgut (Figure 2A).

Given that uracil-induced *Hh* expression and DUOX activation was observed in the anterior midgut regions, we investigated the relationship between Hh signaling and DUOX-dependent ROS generation in this region. For this, we used flies carrying inactive Hh signaling ($Hh^{Inactive}$ flies), including the RNAi-based knockdown (KD) flies for *Hh*, *Smoothened* (*Smo*, a G protein-coupled receptor involved in Hh signaling activation), and *Cubitus interruptus* (*Ci*, an Hh signaling-activated zinc finger-containing transcription factor) (Lum and Beachy, 2004). The uracil-induced DUOX activation in all of these $Hh^{Inactive}$ flies was determined by detecting DUOX-dependent ROS generation using a specific R19S dye (Chen et al., 2011). The result showed that uracil-dependent ROS generation was almost completely abolished in these $Hh^{Inactive}$ flies (Figures 2B and S2A). In contrast, when we used flies carrying constitutively active Hh signaling (Hh^{Active} flies), including RNAi-based KD flies for *Costal-2* (*Cos*, a scaffold protein that negatively regulates Hh signaling) (Figure S2A), we found constitutive ROS generation even in the absence of uracil

(C) mRNA-seq reads of genes involved in Hh signaling pathway. *WntD*, *Rab23*, and *Cad99C* are shown at 16 hr in the absence (blue) or presence (red) of uracil treatment.

(D) Modulation of Hh signaling pathway components by uracil treatment. Among 17 genes involved in Hh signaling pathway, 14 genes (indicated by orange box) are found to be inducible at different time points following uracil treatment (Figure S1A). See also Figure S1 and Table S1, Table S2, Table S3, Table S4, and Table S5.

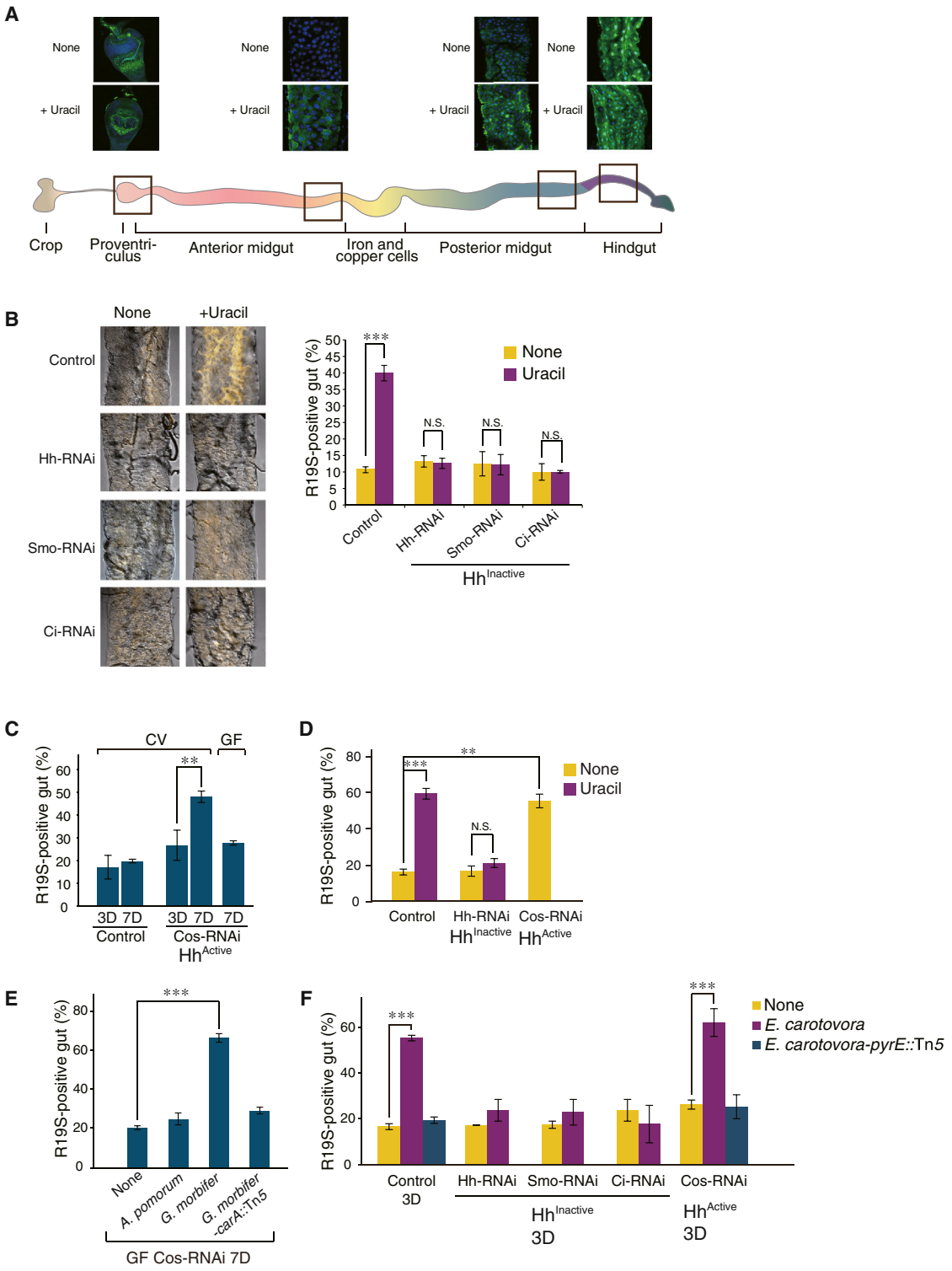

Figure 2. Hh Signaling Is Required for DUOX Activation

(A) Uracil induces *Hh* gene expression. *Hh* gene expression was examined by using flies carrying *Hh-GAL4>UAS-GFP* following 16 hr of uracil ingestion. GFP was visualized by anti-GFP antibody staining. Nuclear staining was performed with DAPI.

(B) Uracil-induced DUOX activation was abolished in $Hh^{Inactive}$ flies. Adult flies (3-day-old) were orally administered with uracil (20 nM) for 90 min, and DUOX-dependent ROS production in the midgut was visualized by HOCl-specific R19S dye (orange). Representative confocal microscopic images and percentage of ROS-positive intestines were shown.

(legend continued on next page)

ingestion under a conventional (CV) condition, i.e., in the presence of commensal and environmental bacteria (Figure 2C). Interestingly, the constitutive ROS generation was not evident in the 3-day-old Hh^{Active} flies, but it then became evident in 7-day-old Hh^{Active} flies (Figure 2C), although the KD effect of *Cos* was similar in the 3-day-old and 7-day-old flies (Figure S2A). Conditional activation or inactivation of Hh signaling in enterocytes using *NP1-GAL4*^{ts} (combining *NP1-GAL4* and the temperature-sensitive GAL4 inhibitor *tub-GAL80*^{ts}) also gave similar results (Figure 2D). These results suggest that an increased and/or accumulated bacterial burden in 7-day-old flies may have led to the constitutive ROS generation in the presence of constitutive Hh signaling activation. In fact, we found that this high constitutive ROS level was completely abolished in the germ-free (GF) Hh^{Active} flies (Figure 2C), indicating that Hh signaling activation alone is not sufficient, but requires bacterial-derived ligands, to induce DUOX activation.

Bacterial-Derived Uracil Induces DUOX Activation through Hh Signaling

As high constitutive ROS levels seen in Hh^{Active} animals were completely abolished in the GF condition, we investigated whether bacterial-derived uracil was responsible for DUOX activation. For this, DUOX-dependent ROS generation was examined in Hh^{Active} GF flies that were previously mono-associated with bacteria possessing various levels of uracil production. The results showed that uracil-producing bacteria induced a high level of intestinal ROS generation, whereas bacteria with reduced uracil-producing abilities showed a low basal level of ROS (Figure 2E). Consistently, *E. carotovora*, but not its uracil auxotrophic mutant, induced DUOX activation in a Hh signaling-dependent manner (Figure 2F). Taken together, these results indicate that bacterial-derived uracil is responsible for DUOX-dependent ROS generation via Hh signaling activation.

Uracil Induces Intestinal *Cad99C* Expression in a Hh Signaling-Dependent Manner

We next investigated the molecular mechanism by which Hh signaling mediates uracil-induced DUOX activation. RNA-Seq and real-time qPCR analyses showed that *Cad99C* was significantly induced among the uracil-induced Hh target genes (Figures 1C and S1A). The cadherin family is comprised of calcium-dependent cell adhesion molecules involved in various biological processes, such as epithelial cell integrity and polarity (Niessen et al., 2011). Cad99C, one of 17 cadherin-like protein members in the cadherin family, was shown to be involved in microvilli morphogenesis in *Drosophila* follicle cells (D'Alterio et al., 2005; Schlichting et al., 2006). Previously, it was shown that *Cad99C* expression is controlled by Ci in the Hh signaling pathway in the wing imaginal disc (Schlichting et al., 2005). When we examined *Cad99C* expression following uracil stimulation, we found that uracil-induced *Cad99C* expression was abolished in all $Hh^{Inactive}$ flies, whereas constitutive *Cad99C* expression (in the absence of uracil stimulation) was observed in Hh^{Active} flies (Figure 3A). As expected, similar Hh signaling-dependent expression patterns were also observed in other Hh target genes, such as *WntD*, *Wnt6*, and *Dpp* (Figure S2B). Based on these observations, we conclude that uracil induces intestinal *Cad99C* expression in a Hh signaling-dependent manner.

Hh-Dependent *Cad99C* Expression Is Required for DUOX Activation

We next investigated the molecular relationship between *Cad99C* induction and DUOX-dependent ROS generation. When we examined the intestinal ROS levels in flies having *Cad99C* overexpression in their enterocytes, we found a high basal level of ROS generation in 7-day-old but not 3-day-old flies (Figure 3B), which is a similar situation to that observed in the case of the 3-day-old versus 7-day-old Hh^{Active} flies (Figure 2C). These results suggest that low levels of uracil are secreted by the conventional microbiota community, which is sufficient in activating DUOX in a specific genetic condition (e.g., Hh^{Active} or *Cad99C*-overepxressing animals), but not sufficient for DUOX activation in a wild-type genetic background. Importantly, the constitutive ROS generation observed in the 7-day-old Hh^{Active} flies was completely abolished in the absence of *Cad99C*, indicating that Hh-induced ROS generation requires *Cad99C* (Figure 3C). Consistent with this result, *Cad99C* mutant flies were unable to induce uracil-dependent ROS generation, whereas enterocyte-specific reintroduction of *Cad99C* in the *Cad99C* mutants conferred the ability to produce uracil-induced ROS generation (Figure 3D). Taken together, these results demonstrate that Cad99C acts as an essential downstream component of the Hh signaling pathway in uracil-induced DUOX activation and ROS generation in gut epithelia of *Drosophila*.

Cad99C Clustering in Enterocyte Membrane Is Required for DUOX Activation

To further investigate the molecular mechanism by which Cad99C participates in uracil-induced DUOX activation, we first examined the membrane localization of endogenous Cad99C in

(C) Gain of function of Hh signaling induces constitutive ROS production. *Cos-RNAi* flies were used as Hh^{Active} flies. Germ-free (GF) and conventionally reared (CV) flies were used. The ages of flies were indicated: 3-day-old (3D) and 7-day-old (7D). Percentage of ROS-positive intestines was shown.

(D) Hh signaling in enterocytes is involved in DUOX-dependent ROS generation. Conditional activation or inactivation of Hh signaling in the enterocytes was performed by using *NP1-GAL4*^{ts}, and 7-day-old flies were used. Flies were kept at 18°C (permissive temperature), then shifted to 29°C during the adult stage to allow expression of the transgenes. Percentage of ROS-positive intestines was shown.

(E and F) Bacterial-derived uracil is responsible for DUOX-dependent ROS generation via Hh signaling activation. GF *Cos-RNAi* flies were mono-associated with bacteria with uracil-producing ability (*G. morbifer*) or bacteria with reduced uracil-producing ability (*A. pomorum* or *G. morbifer-carA*::Tn*5*), and DUOX-dependent ROS production was examined by R19S dye (E). CV adult flies of different genotypes (Control, Hh^{Active} or $Hh^{Inactive}$) were orally administered with ~1 × 10^9 cells of *E. carotovora* or *E. carotovora-pyrE*::Tn*5* for 90 min, and DUOX-dependent ROS production was examined by R19S dye (F). Percentage of ROS-positive intestines was shown. The ages of flies were indicated: 3-day-old (3D) and 7-day-old (7D).

Data were analyzed using an ANOVA followed by Tukey post hoc test (B, C, E, and F) or by Tamhane's T2 post hoc test (D); values represent mean ± SEM (**$p < 0.005$, ***$p < 0.001$) of at least three independent experiments. N.S. denotes not significant.

See also Figure S2 and Table S6.

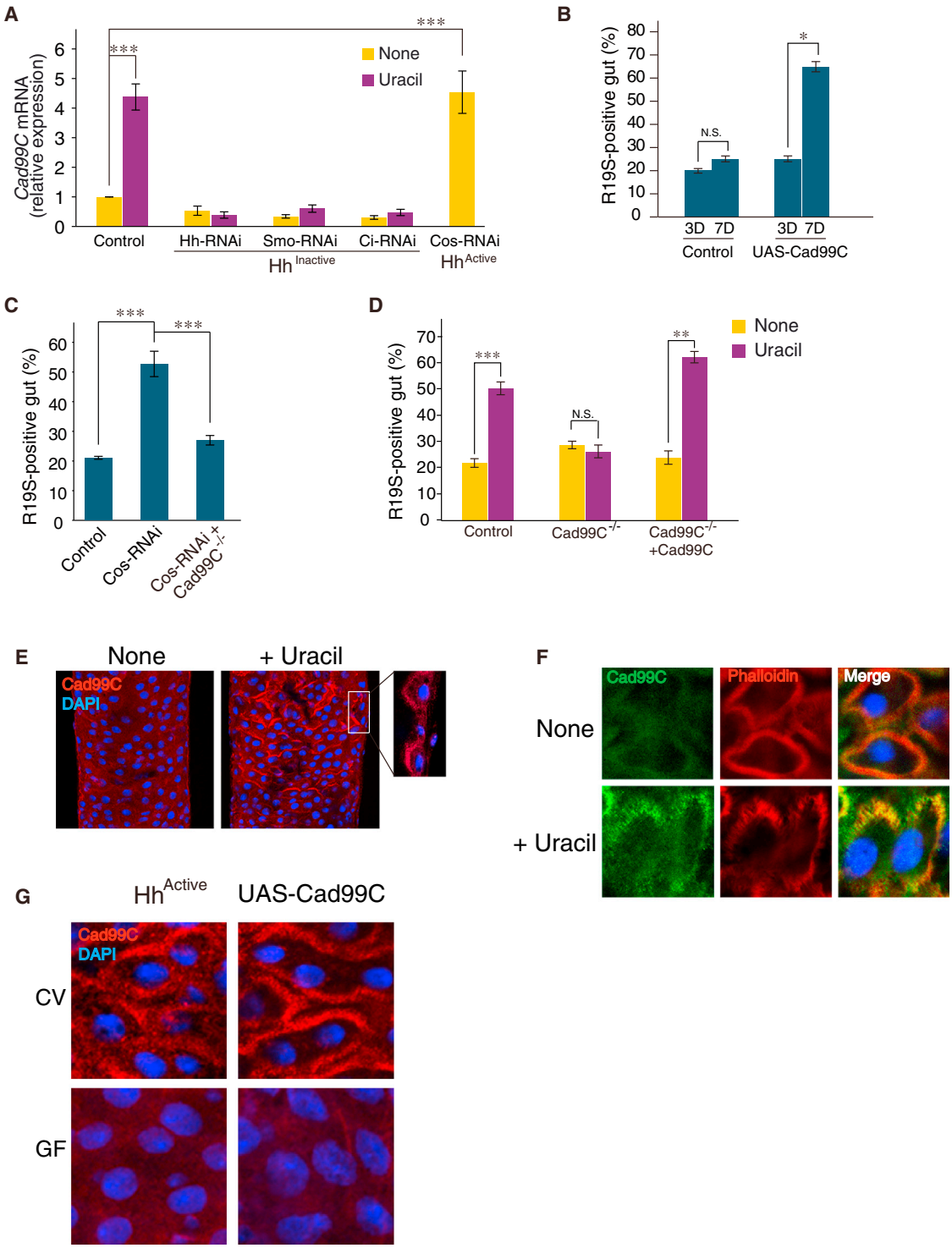

Figure 3. Hh-Dependent *Cad99C* Induction and Its Clustering Are Required for DUOX Activation

In the case of uracil stimulation, flies were subjected to uracil ingestion (20 nM) for 2 hr (A) and 90 min (D–F).

(A) Uracil induces *Cad99C* expression via Hh signaling activation. The expression levels of *Cad99C* were analyzed in anterior midguts obtained from different flies (7-day-old) following uracil ingestion. Target gene expression in the untreated control flies was taken arbitrarily as 1, and the results were shown as relative levels of expression. T bars, means ± SEM (***$p < 0.001$) of at least three independent experiments.

(B) *Cad99C* overexpression is sufficient to induce constitutive ROS generation. Percentage of ROS-positive intestines was shown. The ages of flies (3D or 7D) were indicated.

(C) Constitutive ROS generation in Hh^{Active} flies was abolished in the absence of Cad99C. Percentage of ROS-positive intestines (7-day-old) was shown.

(legend continued on next page)

the presence or absence of uracil stimulation by generating an anti-Cad99C antibody. Immunostaining analysis revealed that endogenous Cad99C is highly dispersed throughout the membrane, which is difficult to observe in the absence of uracil stimulation (Figure 3E). Importantly, Cad99C clustering rapidly became evident throughout the enterocyte membrane following uracil stimulation (Figure 3E). Under this condition, endogenous Cad99C was colocalized with phalloidin, a marker of the brush border membrane (Figure 3F). When we examined Cad99C localization in 7-day-old Hh^{Active} flies or Cad99C-overexpressing flies, we found constitutive Cad99C clustering under a CV condition, which was completely abolished under a GF condition (Figure 3G). These results indicate that either constitutive Hh signaling activation or Cad99C overexpression is sufficient to induce Cad99C clustering under a CV condition.

Cad99C-Dependent Endosome Formation Is Required for DUOX Activation

When we overexpressed *Cad99C* using *Cad99C-GFP* transgenic flies under a CV condition, Cad99C-GFP was found to be intensively clustered in the apical membrane, with multiple foci in the enterocyte cytoplasm in the 7-day-old flies and, to a lesser extent, the 3-day-old flies (Figure 4A). In the case of the 3-day-old flies, uracil stimulation further enhanced Cad99C-GFP localization into multiple foci inside the cells (Figure 4B). To see whether uracil-induced Cad99C foci formation is dependent on endocytosis, flies were administered uracil together with chlorpromazine (CPZ), an inhibitor of clathrin-mediated endocytosis. In this case, the uracil-induced Cad99C foci formation was completely abolished (Figure 4B). Similar results were observed when endocytosis in the enterocyte was genetically blocked by overexpressing a temperature-sensitive allele of *shibire* (*shibire*^{ts}) (Figure 4B). Furthermore, endogenous Cad99C was most intensively colocalized with the endocytosis marker Rab7 upon uracil stimulation (Figure 4C). Importantly, the uracil-induced $Rab7^{+}$ endosome formation was completely abolished in *Cad99C* mutant flies (Figure 4D). Furthermore, we found that 7-day-old Hh^{Active} flies exhibited spontaneous $Rab7^{+}$ endosome formation under a CV condition, which was greatly attenuated under a condition of *Cad99C-KD* (Figure 4E). These results demonstrate that uracil induces endosome formation in a Cad99C-dependent manner. Several lines of evidence have suggested that the ligand-induced endosome acts as a platform to facilitate the intracellular signaling relay (McShane and Zerial, 2008; Miaczynska et al., 2004). In support of this notion, blocking endosome formation either by CPZ treatment or by overexpressing *shibire*^{ts} is sufficient to abolish uracil-induced ROS generation (Figure 4F). As uracil-induced endosome formation is absent in *Cad99C* mutant flies, we concluded that Cad99C is required for the uracil-induced endosome formation that is an essential event in DUOX-dependent ROS generation.

PKC Is Required for Cad99C-Dependent Endosome Formation and Subsequent DUOX Activation

We next examined the molecular mechanism by which Cad99C mediates uracil-induced endosome formation. The Cad99C protein is composed of a long extracellular region, a transmembrane region, and a short cytoplasmic region (D'Alterio et al., 2005). When the mutant form of Cad99C lacking the cytoplasmic region (Cad99CΔcyto-GFP) was overexpressed, we found that Cad99C-dependent endosome formation was completely abolished (Figure 5A). Structure analysis showed that the cytoplasmic region of Cad99C has a binding motif for PSD-95/Discs-large/ZO-1 (PDZ) domain, referred to as PDZ-binding motif. The PDZ-binding motif allows an association with PDZ domain of a scaffold protein in order to form a protein complex (Demontis et al., 2006). Previously, we reported that phospholipase Cβ (PLCβ) is the key component in the DUOX-activity pathway (Ha et al., 2009a). Given that PLCβ is known to act as an upstream activator of protein kinase C (PKC) (Rhee, 2001), and that both proteins contain PDZ-binding motif(s), we investigated the possible involvement of PKC in Cad99C-dependent endosome formation. Real-time qPCR analyses revealed that *PKC1* and *PKC2* are inducible in response to uracil stimulation (Figure 5B). To observe the PKC activation in vivo, we generated transgenic flies that expressed PKC2 fused to red fluorescence protein (RFP), because activated PKC is known to be localized in the membrane region of the cells (Rosse et al., 2010). Using these flies, we observed that uracil stimulation activates PKC2 in the enterocytes (Figure 5C). We further found that PKC2 is rapidly localized with the Cad99C-dependent $Rab7^{+}$ endosomes following uracil stimulation (Figure 5D). Importantly, uracil-induced Cad99C clustering and Cad99C-dependent $Rab7^{+}$ endosome formation were abolished in the PKC1/2-KD flies (Figure 5E), indicating that PKC is required for uracil-induced Cad99C activation and subsequent endosome formation. Furthermore, uracil-induced ROS generation was abolished in PKC1/2-KD flies (Figure 5F). These results indicate that both PKC and Cad99C are required for uracil-induced endosome formation and subsequent DUOX activation.

Reciprocal Activation of PLCβ and Cad99C in Endosomes Is Required for DUOX Activation

Given that PLCβ is the key component of the DUOX-activity pathway (Ha et al., 2009a) and is known to act as an upstream activator of PKC (Rhee, 2001), we investigated the involvement of PLCβ on Cad99C activation. Upon uracil stimulation, we found that PLCβ is rapidly localized with the Cad99C-dependent

(D) Cad99C is required for uracil-induced ROS generation. *Cad99C*$^{-/-}$ flies (3-day-old) were genetically rescued by enterocyte-specific expression of *Cad99C* (Cad99C$^{-/-}$ + Cad99C). Percentage of ROS-positive intestines was shown.
(E) Uracil stimulation induces Cad99C clustering.
(F) Cad99C colocalized with phalloidin in response to uracil.
(G) Spontaneous Cad99C clustering was observed in animals carrying constitutive Hh signaling (Hh^{Active}) or animals carrying *Cad99C* overexpression (UAS-Cad99C) under the CV condition, but not the GF condition. Seven-day-old flies were used.
Data were analyzed using an ANOVA followed by Tukey post hoc test (B and C) or by Tamhane's T2 post hoc test (D); values represent mean ± SEM (*$p < 0.05$, **$p < 0.005$, ***$p < 0.001$) of at least three independent experiments. N.S. denotes not significant.
See also Table S5 and Table S6.

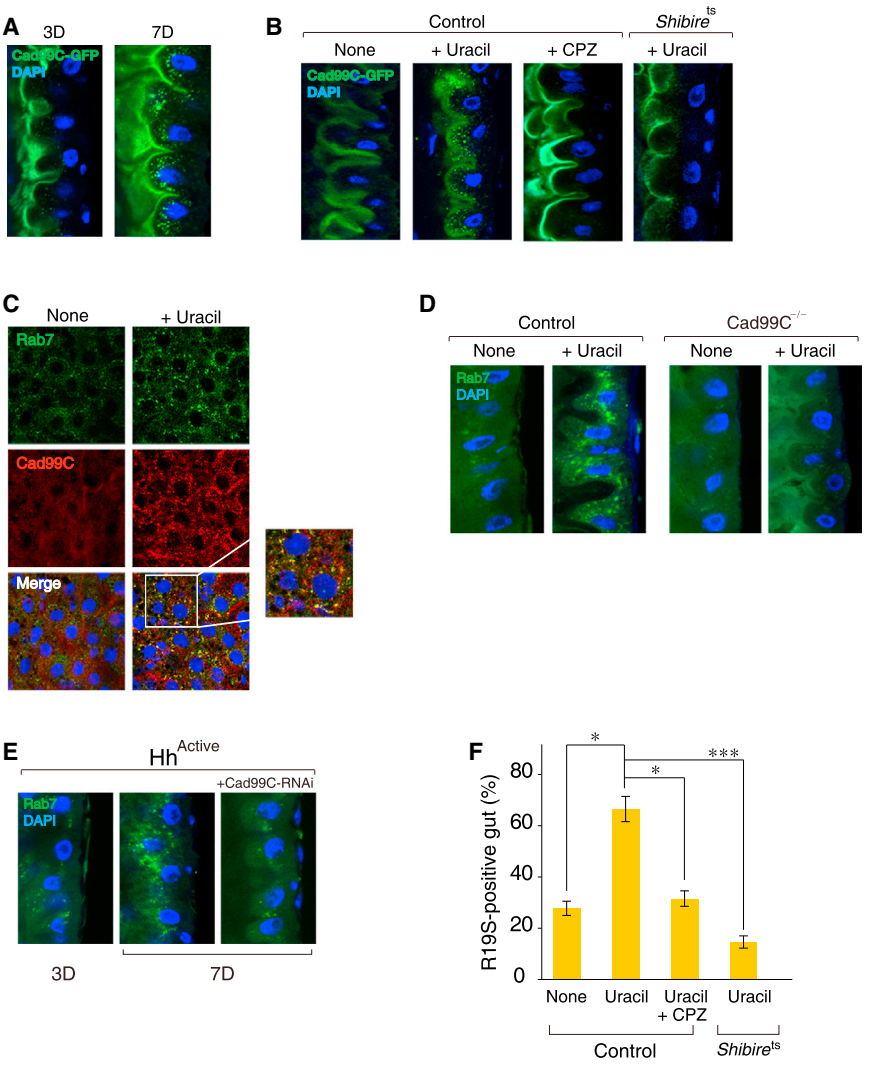

Figure 4. Cad99C-Dependent Endosome Formation Is Required for Uracil-Induced ROS Generation

In the case of uracil stimulation, flies were subjected to uracil ingestion (20 nM) for 90 min.

(A) *Cad99C* overexpression leads to Cad99C-positive foci formation in the cytoplasmic region of enterocytes in the absence of uracil stimulation. *NP1-GAL4>UAS-Cad99C-GFP* flies in different ages (3D or 7D) were used.

(B) Endocytosis is required for uracil-induced Cad99C-positive foci formation. Flies (3-day-old) were used and endocytosis was blocked chemically (by preingestion of 10 μM of chlorpromazine [CPZ] for 30 min before uracil ingestion) or genetically (by overexpressing *shibire*^{ts}, a temperature-sensitive allele of *shibire*). Flies were kept at 18°C (permissive temperature), then shifted to 29°C for 1 hr before uracil ingestion.

(C) Cad99C-positive foci were largely colocalized with Rab7-positive endosomes. YFP was visualized by antibody staining using Rab7-YFP flies.

(D) Cad99C is required for uracil-induced Rab7-positive endosome formation.

(E) Constitutive endosome formation in Hh^{Active} flies was abolished in the presence of *Cad99C-RNAi*. Hh^{Active} flies (*HS-GAL4>UAS-Hh*) in different ages (3D or 7D) were used. Adult flies were maintained at 29°C to induce constitutive *Hh* induction.

(F) Endosome formation is required for uracil-induced ROS generation. Endocytosis was blocked chemically or genetically as described in (B). Percentage of ROS-positive intestines was shown. Data were analyzed using an ANOVA followed by Tamhane's T2 post hoc test; values represent mean ± SEM (*$p < 0.05$, ***$p < 0.001$) of at least three independent experiments.

See also Table S6.

Rab7$^+$ endosomes (Figure 5G). Furthermore, we also found that uracil-induced Cad99C clustering and Cad99C-dependent Rab7$^+$ endosome formation were abolished in *PLCβ* mutant flies (Figure 5H), indicating that PLCβ activity is required for uracil-induced Cad99C activation and subsequent endosome formation. Previously, we showed that PLCβ-dependent Ca^{2+} mobilization is essential for DUOX activation (Ha et al., 2009a). *Cad99C* overexpression induced PLCβ-dependent Ca^{2+} mobilization under a CV condition (Figure 5I). Furthermore, uracil-induced and PLCβ-dependent Ca^{2+} mobilization was abolished in *Cad99C* mutant flies (Figure 5J). Therefore, it is likely that reciprocal activation takes place between PLCβ and Cad99C (Figures 5H and 5J), an event which is required for uracil-induced endosome formation and subsequent DUOX activation.

Hh Signaling Activation and Cad99C-Dependent Endosome Formation Are Required for Host Resistance to Gut Infection

Genetic analyses revealed that two DUOX-regulatory pathways function in efficient pathogen-induced ROS production via the "DUOX-activity pathway," involving Gαq-PLCβ-Ca^{2+}-mediated signaling that modulates DUOX enzymatic activity, and the "*DUOX*-expression pathway," that modulates *DUOX* gene induction through the sequential activation of MEKK1-MKK3-p38 MAPK (Ha et al., 2009a, 2009b). When we examined all of these DUOX-activating signaling events in Hh^{Inactive} flies, we found that these Hh^{Inactive} flies were unable to mount Cad99C clustering (Figure 6A), Cad99C-dependent Rab7$^+$ endosome formation (Figure 6B), PLCβ-dependent Ca^{2+} mobilization (Figure 6C), and p38 MAPK activation (Figure 6D) in response to uracil stimulation. Such signaling defects found in Hh^{Inactive} flies resulted in the inability of uracil-induced ROS production (Figure 6E), leading to an elevated rate of mortality following gut infection (Figure 6F). Given that Hh controls uracil-induced *Cad99C* expression and that Cad99C is an essential element for PLCβ activation, we tested whether the ectopic expression of *Cad99C* expression in the Hh^{Inactive} flies would restore uracil-induced DUOX activation. The result showed that gut-specific reintroduction of *Cad99C* expression into Hh^{Inactive} flies is sufficient to restore all of the signaling events necessary for

DUOX activation (Figures 6A–6E). Consistently, the low level of uracil-induced p38 MAPK activation observed in *Smo* mutant clones was completely restored to the normal level by ectopic expression of *Cad99C* (Figure S3), indicating that Hh signaling is operating in a cell-autonomous manner to maintain proper *Cad99C* expression for DUOX-activating signaling. Furthermore, the high infection-induced lethality found in all $Hh^{Inactive}$ flies was rescued by the enterocyte-specific overexpression of *Cad99C* (Figure 6F). These results demonstrated that the lethality of $Hh^{Inactive}$ flies is due to a reduced level of *Cad99C* expression, and that normal *Cad99C* expression regulated by the Hh pathway and Cad99C-dependent signaling endosome formation are all essential events for the DUOX-dependent gut immunity that is required for resisting pathogen infection.

DISCUSSION

Hh signaling is an evolutionarily conserved signaling pathway that is well-known to be involved in embryonic patterning and organogenesis (Lum and Beachy, 2004; Varjosalo and Taipale, 2008). Hh signaling also plays an important role in development and homeostasis of adult organs such as the gastrointestinal (GI) tract in *Drosophila* and mammals (Huangfu and Anderson, 2006; Singh et al., 2011; Takashima et al., 2008). In the *Drosophila* adult GI tract, Hh was recently shown to be required for the differentiation of stem cells in the hindgut and proventriculus (Singh et al., 2011; Takashima et al., 2008). In addition to developmental process, previous microarray analysis showed that the Hh ligand in the adult gut is induced following bacterial infection (Buchon et al., 2009), although the exact role of Hh signaling during infection remains to be determined.

In this study, an unexpected role for Hh signaling in *Drosophila* gut innate immunity was found. Our analysis showed that bacterial-derived uracil induces *Hh* expression and that this Hh signaling in turn induces enterocyte *Cad99C* expression. Given that uracil-induced DUOX activation was abolished in $Hh^{Inactive}$ flies, and that overexpression of *Cad99C* in the $Hh^{Inactive}$ flies restored uracil-induced DUOX activation, an appropriate level of *Cad99C* induced by Hh signaling is of central importance for DUOX activation. Interestingly, Hh^{Active} animals exhibited spontaneous DUOX activation under a CV condition. However, overactivation of Hh signaling is not sufficient to induce ROS generation, because flies expressing excessive amounts of Hh target genes (such as Hh^{Active} flies, *Cad99C*-overexpressing flies, or both) were unable to induce DUOX activation under a GF condition (Figure S4A). Uracil stimulation rapidly induced DUOX activation of these GF animals (Figure S4A), indicating that uracil recognition (presumably by GPCR that acts with Cad99C) acts as a downstream event of Hh signaling. Further investigations on the identification of uracil receptor(s) will clarify how uracil induces Hh signaling activation and Cad99C-mediated DUOX activation.

How is Cad99C involved in DUOX activation? An interesting aspect of the membrane dynamics upon uracil stimulation is the formation of signaling endosomes. As Cad99C colocalizes with uracil-induced $Rab7^+$ endosomes, it is likely that Cad99C is internalized by endocytosis to form endosomes. It is important to note that uracil-induced endosome formation is abolished in the absence of *Cad99C*, indicating that Cad99C is required for signal-induced endosome formation. Signaling-induced endosomes, so-called "signaling endosomes," have been shown to play an active role in signal propagation and amplification by providing a physical platform to which intracellular signaling molecules are recruited (McShane and Zerial, 2008; Miaczynska et al., 2004). Our results showed that an inhibition of endosome formation using an endocytosis inhibitor abolished uracil-induced DUOX activation, indicating that Cad99C-mediated endosome formation is required for the signaling activation that in turn results in DUOX activation. In this regard, it is interesting to note that Cad99C and PLCβ/PKC exhibited reciprocal activation (Figure 5), and overexpression of one of these components induced spontaneous ROS generation under a condition of increased intestinal bacterial burden, i.e., intestines of 7-day-old flies (Figures S4A and S4B). Furthermore, Cad99C colocalized with PLCβ upon uracil stimulation (Figure S4C). Cad99C, PKC, and PLCβ are known to contain PDZ-binding motif(s). It is well-known that the PDZ-binding motif of different proteins can directly bind to the PDZ domain of a scaffold protein. One such example is the inaD protein that contains multiple PDZ domains; this protein acts as a scaffold that recruits different signaling molecules, each of which has a PDZ-binding motif(s) (van Huizen et al., 1998). Therefore, it may be possible that Cad99C, PKC, and PLCβ bind to a scaffold protein containing multiple PDZ domains. However, identification of such scaffold protein remains to be elucidated to definitely prove this mechanism.

Interestingly, the uracil auxotrophic mutant of *E. carotovora* can induce *Hh* ligand expression in the midgut (Figure S4D); however, this bacterial strain is incapable of generating DUOX-dependent ROS (Figure 2F). Consistently, PG ingestion effectively activated Hh signaling (Figures S4E and S4F). These results indicate that two important bacterial ligands, uracil and PG, independently induce Hh signaling. Previous reports have shown that, unlike uracil, PG alone does not induce DUOX activation (Ha et al., 2009a, 2009b). Consistent with this observation, we found that PG alone did not induce Cad99C clustering and Cad99C-dependent endosome formation (Figures S4G and S4H). This is probably due to the fact that, unlike uracil, PG alone does not induce PLCβ-dependent Ca^{2+} mobilization (Figure S4I), which is necessary for Cad99C clustering and signaling endosome formation. At present, it is unclear how PG and uracil induce *Hh* expression. Previously, it has been shown that both ligands independently induce MEKK1 activation leading to ATF2-dependent *DUOX* gene expression (Ha et al., 2009b). Therefore, it is tempting to speculate that the same pathway may be also involved in both uracil- and PG-induced *Hh* ligand expression. Further studies will be needed to understand the exact role of ATF2 in intestinal *Hh* expression.

As PLCβ/PKC activity is essential for activating the DUOX-activity pathway and *DUOX*-expression pathway, it is likely that Cad99C-containing endosomes recruit PLCβ and PKC for the signaling that results in Ca^{2+}-dependent DUOX activity (Figure 7). Once activated, DUOX-dependent gut immunity needs to be negatively regulated, because excess ROS production is deleterious to the host via oxidative damage. $Rab7^+$ late phase endosomes are known to fuse with lysosomes and become degraded (Luzio et al., 2007), suggesting that $Cad99C^+$ $Rab7^+$ endosomes are rapidly fused to lysosomes for their degradation

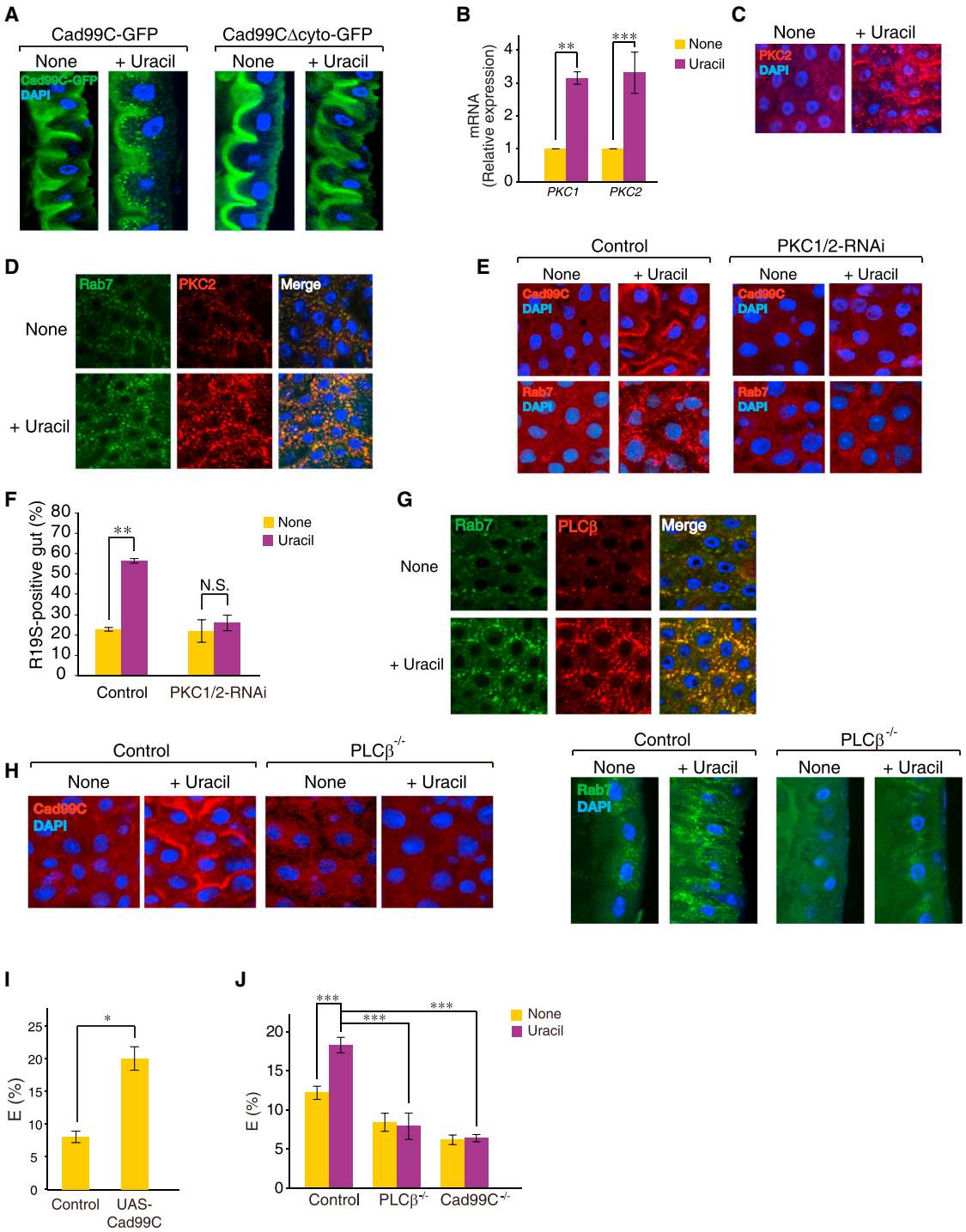

Figure 5. PKC and PLCβ Are Required for Cad99C-Dependent Endosome Formation and Subsequent DUOX Activation

In the case of uracil stimulation, flies were subjected to uracil ingestion (20 nM) for 90 min (A and C–H), 2 hr (B), or 45 min (J).

(A) Cytoplasmic domain of Cad99C is required for uracil-induced endosome formation. *Cad99C-GFP* and *Cad99CΔcyto-GFP* flies were used.

(B) *PKC* genes are induced following uracil stimulation. Quantitative RT-PCR of *PKC1* and *PKC2* was performed with midgut epithelia following uracil stimulation. Target gene expression in the absence of uracil treatment was taken arbitrarily as 1, and the results were shown as relative levels of expression. T-bars, means ± SEM (**p < 0.005, ***p < 0.001) of at least three independent experiments.

(C) Activation of PKC2 can be observed in the gut following uracil stimulation. Transgenic flies carrying *PKC2-RFP* were used to monitor the membrane-targeted activated-form of PKC2.

(D) PKC2 was colocalized with Rab7-positive endosomes following uracil stimulation.

(legend continued on next page)

to downregulate DUOX-dependent ROS generation (Figure 7). Consistent with this notion, inhibition of lysosome function by feeding animals with chloroquine is sufficient to induce spontaneous Cad99C^{+} endosome formations and constitutive ROS production even in the absence of uracil ingestion under a CV condition (Figure S5), which is similar to that observed in CV Hh^{Active} flies. Therefore, the signaling endosome formation/degradation process likely determines the duration and intensity of DUOX activation for the purpose of maintaining the homeostasis of gut immunity.

Drosophila Cad99C is most closely related to vertebrate protocadherin 15 (PCDH15) protein (D'Alterio et al., 2005). Because our preliminary data showed that PCDH15 is required for uracil-induced ROS generation in human intestinal cell lines (Figure S6), the role of Cad99C in DUOX activation is apparently conserved from *Drosophila* to mammals. However, further studies are necessary to see whether Hh signaling pathway mediates *PCDH15* expression.

Recently, a commensal strain, *Lactobacillus plantarum*, has been reported to induce NOX-dependent ROS generation in murine and *Drosophila* intestines (Jones et al., 2013), which is important for the proliferation of intestinal stem cells. These data, together with those of the present study, indicate that different bacterial strains activate a distinct member of the NADPH oxidase family in the gut to control a diverse range of host physiologies. Future elucidation of the molecular mechanisms of intestinal ROS generation by different bacterial strains will provide insights into redox-modulated gut-microbe homeostasis.

EXPERIMENTAL PROCEDURES

In Vivo ROS Measurement

To measure DUOX-dependent ROS generation in vivo, HOCl-specific rhodamine-based R19S dye was used exactly as described previously (Chen et al., 2011).

Immunostaining

Adult flies of different genotypes were orally administered 5% sucrose solution containing uracil (20 nM) for 1.5 hr. The anterior midguts were dissected in PBS and then fixed for 15 min with 4% paraformaldehyde. Samples were washed three times for 5 min with 0.1% Triton X-100 in PBS and incubated with the same solution supplemented with 5% bovine serum albumin for 20 min. Anti-Cad99C polyclonal rabbit antibody was generated by using a synthetic peptide corresponding to amino acid residues 1,691–1,706 of Cad99C as described previously (Schlichting et al., 2005). The samples were incubated with anti-Cad99C antibody (1:500 dilution), anti-Rab7 antibody (1:500 dilution; Abcam), the phospho-specific anti-p38 antibody (1:500 dilution; Millipore, Milford, MA, USA), anti-PLCβ antibody (1:100 dilution; BD Biosciences), anti-GFP antibody (1:1,000 dilution; Life Technologies), or anti-Alexa Fluor 568 phalloidin (1:1,000 dilution; Life Technologies) for 16 hr at 4°C. The samples were then washed five times for 5 min with 0.1% Triton X-100 in PBS, and Alexa Fluor 568 goat anti-rabbit IgG or Alexa Fluor 488 goat anti-rabbit or anti-mouse IgG (Invitrogen) was used as the secondary antibody. Following three washes with PBS for 5 min each, the samples were mounted in mounting buffer (Vectorshield, Vector Laboratories Inc., Burlingame, CA, USA). In all cases, upper region of the copper cells, equivalent to R2b and R2c subdomains (Buchon et al., 2013b), was analyzed by confocal microscopy LSM 700 (Carl Zeiss, Oberkochen, Germany). Nuclear staining was performed with DAPI.

Real-Time qPCR Analysis

Fluorescence real-time PCR was performed to quantify gene expression, using the double-stranded DNA dye, SYBR Green (Perkin Elmer, Waltham, MA, USA). Primer pairs were used to detect different target gene transcripts (Table S5). SYBR Green analysis was performed using an ABI PRISM 7700 system (PE Applied Biosystems, Foster City, CA, USA) according to the manufacturer's instructions. All samples were analyzed in triplicate, and the levels of detected mRNA were normalized to those of the control. The normalized data were then used to quantify the relative levels of a given mRNA according to the cycling threshold analysis. Target gene expression is presented as relative expression level.

FRET Analysis

The dissected guts of flies expressing cameleon calcium sensor were fixed and plated onto coverslips for FRET analysis using a LSM700 Confocal Microscope (Carl Zeiss, Germany). FRET analysis by the acceptor bleaching method was exactly performed as described previously (Ha et al., 2009a).

Gut Infection and Survival Experiment

E. carotovora were harvested during the late exponential phase by centrifugation, and the bacterial pellets were washed with PBS and suspended in 5% sucrose solution. Adult male flies (5- to 6-day-old) were transferred, without starvation, to a vial containing filter paper hydrated with 5% sucrose solution containing bacterial cells ($\sim 10^{10}$ cells for *E. carotovora*) for continuous bacterial feeding during infection time. Filter paper was changed every day.

Statistical Analysis

Comparisons of two samples were made by Student's t test. Comparisons of multiple samples were made by one-way analysis of variance (ANOVA). The log rank test of the Kaplan-Meier was used for the statistical analysis of fly survival experiments. p values of less than 0.05 were considered statistically significant. SPSS software (Chicago, IL, USA) was used for all analyses.

ACCESSION NUMBERS

The Gene Expression Omnibus accession number for the data reported in this paper is GSE57941.

SUPPLEMENTAL INFORMATION

Supplemental Information includes six figures, six tables, and Supplemental Experimental Procedures and can be found with this article at http://dx.doi.org/10.1016/j.chom.2014.12.012.

(E and F) Uracil-induced Cad99C clustering, Rab7-positive endosome formation, and ROS production were abolished in *PKC1/2-RNAi* flies. Cad99C/Rab7 localization (E) and percentage of ROS-positive intestines (F) were shown.

(G) PLCβ was colocalized with Rab7-positive endosomes following uracil stimulation.

(H) PLCβ is required for uracil-induced Cad99C clustering and Rab7-positive endosome formation.

(I and J) FRET analysis. *Cad99C* overexpression leads to the enhanced PLCβ activation (I). Seven-day-old control and *Cad99C*-overexpressing flies (UAS-Cad99C) were used. Cad99C is required for PLCβ activation (J). PLCβ activity was examined by performing FRET analysis for the Ca^{2+} measurement using flies expressing cameleon calcium sensor. FRET efficiency (*E*%) was expressed as the mean ± SD from at least 30 flies.

Data were analyzed using an ANOVA followed by Tukey post hoc test (F and J) or by Tamhane's T2 *post hoc* test (I); values represent mean ± SEM (*$p < 0.05$, **$p < 0.005$, ***$p < 0.001$) of at least three independent experiments. N.S. denotes not significant.

See also Figure S4, Table S5, and Table S6.

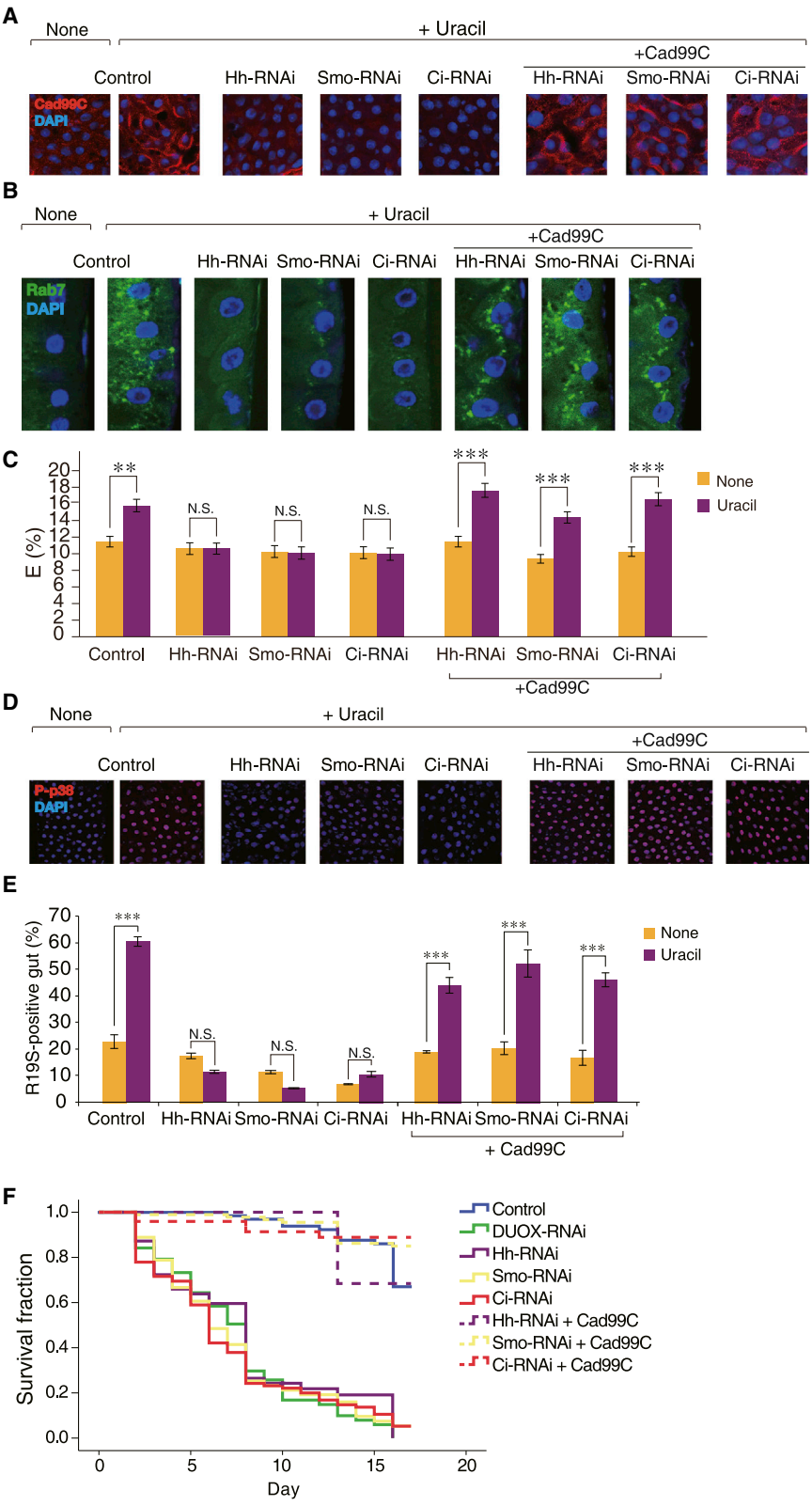

Figure 6. Hh Signaling Activation and Cad99C-Dependent Endosome Formation Are Required for Host Survival against Gut Infection

In the case of uracil stimulation, flies were subjected to uracil ingestion (20 nM) for 90 min (A, B, D, and E) or 45 min (C).

Cad99C clustering (A), Cad99C-dependent Rab7^{+} endosome formation (B), PLCβ-dependent Ca^{2+} mobilization (C), p38 MAPK activation (D), and DUOX-dependent ROS production (E) were examined. Host survival rate following gut infection with *E. carotovora* (F) was also examined. Enterocyte-specific *NP1-GAL4* driver was used in all $Hh^{Inactive}$ flies.

Data were analyzed using an ANOVA followed by Tukey post hoc test (C and E); values represent mean ± SEM (**p < 0.005, ***p < 0.001) of at least three independent experiments. N.S. denotes not significant. For the survival assay (F), a log rank analysis (Kaplan-Meier method) showed a significant difference in survival (p < 0.001) between $Hh^{Inactive}$ flies and genetically rescued $Hh^{Inactive}$ flies expressing *Cad99C*.

See also Figure S3 and Table S6.

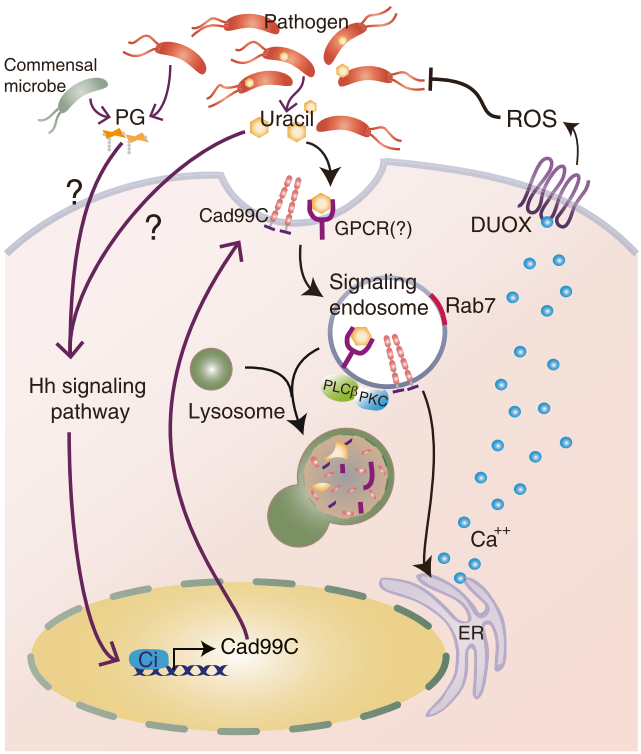

Figure 7. A Model for Hh Signaling and Cad99C-Dependent Signaling Endosome Formation in *Drosophila* DUOX-Dependent Gut Immunity

Uracil or peptidoglycan (PG) released from the pathogens induces the Hh signaling pathway through an unknown mechanism in order to maintain high Cad99C level in the apical membrane. PG molecules from commensal bacteria may also play a role in maintaining the appropriate basal level of Hh-dependent Cad99C under a conventional condition before pathogen infection. When uracil is recognized by a presently unknown G protein coupled receptor (GPCR), Cad99C/PLCβ/PKC-dependent signaling endosomes facilitate the signal amplification by inducing PLCβ-dependent Ca^{2+} mobilization so as to induce DUOX-dependent ROS generation. Signaling endosomes are then subjected to degradation, possibly the endolysosomal pathway, in order to avoid excess ROS generation. See the Discussion section for more detail. See also Figures S4 and S5.

AUTHOR CONTRIBUTIONS

K.-A.L. and B.K. performed most experiments. J.B., E.-K.K., and D.H performed RNA-seq analyses. D.H.K., H.Y., S.-H.K., K.-A.L., B.K., and W.-J.L. conceived the work and evaluated results. J.-H.R. performed PCDH15 experiments. K.-A.L., B.K., and W.-J.L. wrote the manuscript.

ACKNOWLEDGMENTS

This study was supported by the National Creative Research Initiative Program (grant number 2006-0050687 to W.-J.L.) and the Basic Science Research Program (grant numbers NRF-2013R1A1A2013219, NRF-2013R1A1A2013250, and NRF-2013R1A1A2060210 to K.-A.L., S.-H.K., and E.-K.K., respectively) from the National Research Foundation of the Ministry of Science, ICT, and Future Planning of Korea.

Received: May 21, 2014
Revised: October 27, 2014
Accepted: December 10, 2014
Published: January 29, 2015

REFERENCES

Bae, Y.S., Choi, M.K., and Lee, W.J. (2010). Dual oxidase in mucosal immunity and host-microbe homeostasis. Trends Immunol. *31*, 278–287.

Brestoff, J.R., and Artis, D. (2013). Commensal bacteria at the interface of host metabolism and the immune system. Nat. Immunol. *14*, 676–684.

Buchon, N., Broderick, N.A., Poidevin, M., Pradervand, S., and Lemaitre, B. (2009). Drosophila intestinal response to bacterial infection: activation of host defense and stem cell proliferation. Cell Host Microbe *5*, 200–211.

Buchon, N., Broderick, N.A., and Lemaitre, B. (2013a). Gut homeostasis in a microbial world: insights from Drosophila melanogaster. Nat. Rev. Microbiol. *11*, 615–626.

Buchon, N., Osman, D., David, F.P., Fang, H.Y., Boquete, J.P., Deplancke, B., and Lemaitre, B. (2013b). Morphological and molecular characterization of adult midgut compartmentalization in Drosophila. Cell Rep. *3*, 1725–1738.

Charroux, B., and Royet, J. (2012). Gut-microbiota interactions in non-mammals: what can we learn from Drosophila? Semin. Immunol. *24*, 17–24.

Chen, X., Lee, K.A., Ha, E.M., Lee, K.M., Seo, Y.Y., Choi, H.K., Kim, H.N., Kim, M.J., Cho, C.S., Lee, S.Y., et al. (2011). A specific and sensitive method for detection of hypochlorous acid for the imaging of microbe-induced HOCl production. Chem. Commun. (Camb.) *47*, 4373–4375.

D'Alterio, C., Tran, D.D., Yeung, M.W., Hwang, M.S., Li, M.A., Arana, C.J., Mulligan, V.K., Kubesh, M., Sharma, P., Chase, M., et al. (2005). Drosophila melanogaster Cad99C, the orthologue of human Usher cadherin PCDH15, regulates the length of microvilli. J. Cell Biol. *171*, 549–558.

Demontis, F., Habermann, B., and Dahmann, C. (2006). PDZ-domain-binding sites are common among cadherins. Dev. Genes Evol. *216*, 737–741.

Ferrandon, D. (2013). The complementary facets of epithelial host defenses in the genetic model organism Drosophila melanogaster: from resistance to resilience. Curr. Opin. Immunol. *25*, 59–70.

Garrett, W.S., Gordon, J.I., and Glimcher, L.H. (2010). Homeostasis and inflammation in the intestine. Cell *140*, 859–870.

Guo, L., Karpac, J., Tran, S.L., and Jasper, H. (2014). PGRP-SC2 promotes gut immune homeostasis to limit commensal dysbiosis and extend lifespan. Cell *156*, 109–122.

Ha, E.M., Oh, C.T., Bae, Y.S., and Lee, W.J. (2005). A direct role for dual oxidase in Drosophila gut immunity. Science *310*, 847–850.

Ha, E.M., Lee, K.A., Park, S.H., Kim, S.H., Nam, H.J., Lee, H.Y., Kang, D., and Lee, W.J. (2009a). Regulation of DUOX by the Galphaq-phospholipase Cbeta-Ca2+ pathway in Drosophila gut immunity. Dev. Cell *16*, 386–397.

Ha, E.M., Lee, K.A., Seo, Y.Y., Kim, S.H., Lim, J.H., Oh, B.H., Kim, J., and Lee, W.J. (2009b). Coordination of multiple dual oxidase-regulatory pathways in responses to commensal and infectious microbes in drosophila gut. Nat. Immunol. *10*, 949–957.

Hooper, L.V., Littman, D.R., and Macpherson, A.J. (2012). Interactions between the microbiota and the immune system. Science *336*, 1268–1273.

Huangfu, D., and Anderson, K.V. (2006). Signaling from Smo to Ci/Gli: conservation and divergence of Hedgehog pathways from Drosophila to vertebrates. Development *133*, 3–14.

Jones, R.M., Luo, L., Ardita, C.S., Richardson, A.N., Kwon, Y.M., Mercante, J.W., Alam, A., Gates, C.L., Wu, H., Swanson, P.A., et al. (2013). Symbiotic lactobacilli stimulate gut epithelial proliferation via Nox-mediated generation of reactive oxygen species. EMBO J. *32*, 3017–3028.

Kanehisa, M., and Goto, S. (2000). KEGG: kyoto encyclopedia of genes and genomes. Nucleic Acids Res. *28*, 27–30.

Kleino, A., and Silverman, N. (2014). The Drosophila IMD pathway in the activation of the humoral immune response. Dev. Comp. Immunol. *42*, 25–35.

Lee, W.J., and Brey, P.T. (2013). How microbiomes influence metazoan development: insights from history and Drosophila modeling of gut-microbe interactions. Annu. Rev. Cell Dev. Biol. *29*, 571–592.

Lee, W.J., and Hase, K. (2014). Gut microbiota-generated metabolites in animal health and disease. Nat. Chem. Biol. *10*, 416–424.

Lee, K.A., and Lee, W.J. (2014). Drosophila as a model for intestinal dysbiosis and chronic inflammatory diseases. Dev. Comp. Immunol. *42*, 102–110.

Lee, K.-A., Kim, S.-H., Kim, E.-K., Ha, E.-M., You, H., Kim, B., Kim, M.-J., Kwon, Y., Ryu, J.-H., and Lee, W.-J. (2013). Bacterial-derived uracil as a modulator of mucosal immunity and gut-microbe homeostasis in Drosophila. Cell *153*, 797–811.

Lemaitre, B., and Hoffmann, J. (2007). The host defense of Drosophila melanogaster. Annu. Rev. Immunol. *25*, 697–743.

Leulier, F., Parquet, C., Pili-Floury, S., Ryu, J.H., Caroff, M., Lee, W.J., Mengin-Lecreulx, D., and Lemaitre, B. (2003). The Drosophila immune system detects bacteria through specific peptidoglycan recognition. Nat. Immunol. *4*, 478–484.

Ley, R.E., Peterson, D.A., and Gordon, J.I. (2006). Ecological and evolutionary forces shaping microbial diversity in the human intestine. Cell *124*, 837–848.

Lhocine, N., Ribeiro, P.S., Buchon, N., Wepf, A., Wilson, R., Tenev, T., Lemaitre, B., Gstaiger, M., Meier, P., and Leulier, F. (2008). PIMS modulates immune tolerance by negatively regulating Drosophila innate immune signaling. Cell Host Microbe *4*, 147–158.

Littman, D.R., and Pamer, E.G. (2011). Role of the commensal microbiota in normal and pathogenic host immune responses. Cell Host Microbe *10*, 311–323.

Lum, L., and Beachy, P.A. (2004). The Hedgehog response network: sensors, switches, and routers. Science *304*, 1755–1759.

Luzio, J.P., Pryor, P.R., and Bright, N.A. (2007). Lysosomes: fusion and function. Nat. Rev. Mol. Cell Biol. *8*, 622–632.

McFall-Ngai, M., Hadfield, M.G., Bosch, T.C., Carey, H.V., Domazet-Lošo, T., Douglas, A.E., Dubilier, N., Eberl, G., Fukami, T., Gilbert, S.F., et al. (2013). Animals in a bacterial world, a new imperative for the life sciences. Proc. Natl. Acad. Sci. USA *110*, 3229–3236.

McShane, M.P., and Zerial, M. (2008). Survival of the weakest: signaling aided by endosomes. J. Cell Biol. *182*, 823–825.

Miaczynska, M., Pelkmans, L., and Zerial, M. (2004). Not just a sink: endosomes in control of signal transduction. Curr. Opin. Cell Biol. *16*, 400–406.

Niessen, C.M., Leckband, D., and Yap, A.S. (2011). Tissue organization by cadherin adhesion molecules: dynamic molecular and cellular mechanisms of morphogenetic regulation. Physiol. Rev. *91*, 691–731.

Paredes, J.C., Welchman, D.P., Poidevin, M., and Lemaitre, B. (2011). Negative regulation by amidase PGRPs shapes the Drosophila antibacterial response and protects the fly from innocuous infection. Immunity *35*, 770–779.

Rhee, S.G. (2001). Regulation of phosphoinositide-specific phospholipase C. Annu. Rev. Biochem. *70*, 281–312.

Rosse, C., Linch, M., Kermorgant, S., Cameron, A.J., Boeckeler, K., and Parker, P.J. (2010). PKC and the control of localized signal dynamics. Nat. Rev. Mol. Cell Biol. *11*, 103–112.

Royet, J., Gupta, D., and Dziarski, R. (2011). Peptidoglycan recognition proteins: modulators of the microbiome and inflammation. Nat. Rev. Immunol. *11*, 837–851.

Ryu, J.H., Ha, E.M., Oh, C.T., Seol, J.H., Brey, P.T., Jin, I., Lee, D.G., Kim, J., Lee, D., and Lee, W.J. (2006). An essential complementary role of NF-kappaB pathway to microbicidal oxidants in Drosophila gut immunity. EMBO J. *25*, 3693–3701.

Ryu, J.H., Kim, S.H., Lee, H.Y., Bai, J.Y., Nam, Y.D., Bae, J.W., Lee, D.G., Shin, S.C., Ha, E.M., and Lee, W.J. (2008). Innate immune homeostasis by the homeobox gene caudal and commensal-gut mutualism in Drosophila. Science *319*, 777–782.

Schlichting, K., Demontis, F., and Dahmann, C. (2005). Cadherin Cad99C is regulated by Hedgehog signaling in Drosophila. Dev. Biol. *279*, 142–154.

Schlichting, K., Wilsch-Bräuninger, M., Demontis, F., and Dahmann, C. (2006). Cadherin Cad99C is required for normal microvilli morphology in Drosophila follicle cells. J. Cell Sci. *119*, 1184–1195.

Shanahan, F. (2013). The colonic microbiota in health and disease. Curr. Opin. Gastroenterol. *29*, 49–54.

Shin, S.C., Kim, S.H., You, H., Kim, B., Kim, A.C., Lee, K.A., Yoon, J.H., Ryu, J.H., and Lee, W.J. (2011). Drosophila microbiome modulates host developmental and metabolic homeostasis via insulin signaling. Science *334*, 670–674.

Singh, S.R., Zeng, X., Zheng, Z., and Hou, S.X. (2011). The adult Drosophila gastric and stomach organs are maintained by a multipotent stem cell pool at the foregut/midgut junction in the cardia (proventriculus). Cell Cycle *10*, 1109–1120.

Storelli, G., Defaye, A., Erkosar, B., Hols, P., Royet, J., and Leulier, F. (2011). Lactobacillus plantarum promotes Drosophila systemic growth by modulating hormonal signals through TOR-dependent nutrient sensing. Cell Metab. *14*, 403–414.

Takashima, S., Mkrtchyan, M., Younossi-Hartenstein, A., Merriam, J.R., and Hartenstein, V. (2008). The behaviour of Drosophila adult hindgut stem cells is controlled by Wnt and Hh signalling. Nature *454*, 651–655.

Tremaroli, V., and Bäckhed, F. (2012). Functional interactions between the gut microbiota and host metabolism. Nature *489*, 242–249.

Turnbaugh, P.J., Ley, R.E., Mahowald, M.A., Magrini, V., Mardis, E.R., and Gordon, J.I. (2006). An obesity-associated gut microbiome with increased capacity for energy harvest. Nature *444*, 1027–1031.

van Huizen, R., Miller, K., Chen, D.M., Li, Y., Lai, Z.C., Raab, R.W., Stark, W.S., Shortridge, R.D., and Li, M. (1998). Two distantly positioned PDZ domains mediate multivalent INAD-phospholipase C interactions essential for G protein-coupled signaling. EMBO J. *17*, 2285–2297.

Varjosalo, M., and Taipale, J. (2008). Hedgehog: functions and mechanisms. Genes Dev. *22*, 2454–2472.

Vijay-Kumar, M., Aitken, J.D., Carvalho, F.A., Cullender, T.C., Mwangi, S., Srinivasan, S., Sitaraman, S.V., Knight, R., Ley, R.E., and Gewirtz, A.T. (2010). Metabolic syndrome and altered gut microbiota in mice lacking Toll-like receptor 5. Science *328*, 228–231.

Wen, L., Ley, R.E., Volchkov, P.Y., Stranges, P.B., Avanesyan, L., Stonebraker, A.C., Hu, C., Wong, F.S., Szot, G.L., Bluestone, J.A., et al. (2008). Innate immunity and intestinal microbiota in the development of Type 1 diabetes. Nature *455*, 1109–1113.